



# HHS Public Access

Author manuscript

*Nano Lett.* Author manuscript; available in PMC 2022 July 23.

Published in final edited form as:

*Nano Lett.* 2021 November 24; 21(22): 9442–9449. doi:10.1021/acs.nanolett.1c02702.

## Ferumoxylol Nanoparticles Target Biofilms Causing Tooth Decay in the Human Mouth

**Yuan Liu,**

Department of Preventive & Restorative Sciences, School of Dental Medicine and Biofilm Research Laboratories, Levy Center for Oral Health, School of Dental Medicine, University of Pennsylvania, Philadelphia, Pennsylvania 19104, United States

**Yue Huang,**

Biofilm Research Laboratories, Levy Center for Oral Health, School of Dental Medicine and Department of Radiology, Perelman School of Medicine, University of Pennsylvania, Philadelphia, Pennsylvania 19104, United States

**Dongyeop Kim,**

Department of Preventive Dentistry, School of Dentistry, Jeonbuk National University, Jeonju 54869, Korea

**Zhi Ren,**

Biofilm Research Laboratories, Levy Center for Oral Health, School of Dental Medicine and Department of Orthodontics, School of Dental Medicine, University of Pennsylvania, Philadelphia, Pennsylvania 19104, United States

**Min Jun Oh,**

Biofilm Research Laboratories, Levy Center for Oral Health, School of Dental Medicine, Department of Orthodontics, School of Dental Medicine, and Department of Chemical and Biomolecular Engineering, University of Pennsylvania, Philadelphia, Pennsylvania 19104, United States

**David P. Cormode,**

---

**Corresponding Authors:** **Domenick T. Zero** – Department of Cariology, Operative Dentistry and Dental Public Health, School of Dentistry, Indiana University, Indianapolis, Indiana 46202, United States; Phone: 317-274-8822; dzero@iu.edu, **Hyun Koo** – Biofilm Research Laboratories, Levy Center for Oral Health, School of Dental Medicine, Department of Orthodontics, School of Dental Medicine, and Center for Innovation & Precision Dentistry, School of Dental Medicine, School of Engineering and Applied Sciences, University of Pennsylvania, Philadelphia, Pennsylvania 19104, United States; Phone: 215-898-8993; koohy@upenn.edu.

**Author Contributions**

Y.L., D.T.Z., and H.K. conceptualized the study. Y.L., Y.H., D.K., and Z.R. developed and performed the study experiments. Y.L., Y.H., D.K., Z.R., and A.T.H. conducted data analysis. M.J.O. designed, prepared, and analyzed the natural tooth biofilm model. Y.L., D.P.C., D.T.Z., and H.K. wrote, reviewed, and edited the manuscript. D.T.Z. and H.K. supervised the study. All authors have given approval to the final version of the manuscript.

Complete contact information is available at: <https://pubs.acs.org/10.1021/acs.nanolett.1c02702>

The authors declare no competing financial interest.

**Supporting Information**

The Supporting Information is available free of charge at <https://pubs.acs.org/doi/10.1021/acs.nanolett.1c02702>.

Detailed study design, clinical procedures and treatment regimen; biofilm analysis; enamel analysis; *in vitro* experimental methods; statistical analysis method; and additional experimental results (PDF)

Department of Radiology, Perelman School of Medicine and Department of Bioengineering, School of Engineering and Applied Sciences, University of Pennsylvania, Philadelphia, Pennsylvania 19104, United States

**Anderson T. Hara,**

Department of Cariology, Operative Dentistry and Dental Public Health, School of Dentistry, Indiana University, Indianapolis, Indiana 46202, United States

**Domenick T. Zero,**

Department of Cariology, Operative Dentistry and Dental Public Health, School of Dentistry, Indiana University, Indianapolis, Indiana 46202, United States

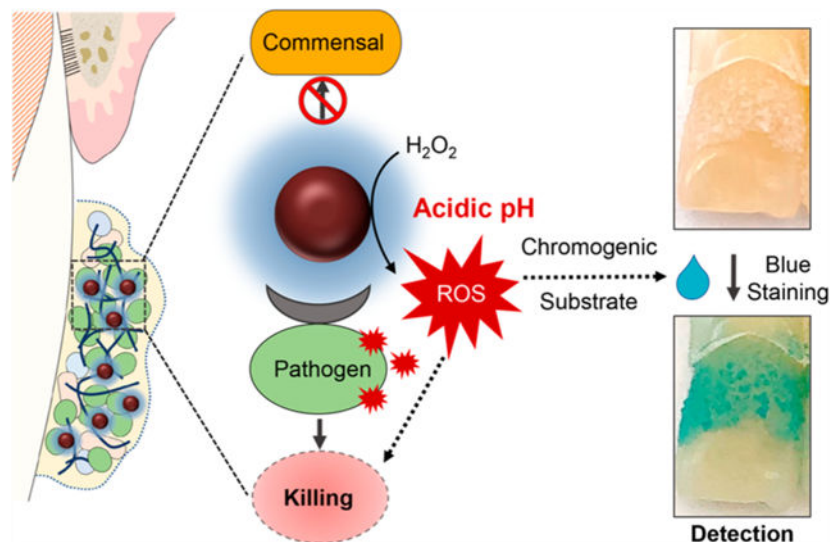
**Hyun Koo**

Biofilm Research Laboratories, Levy Center for Oral Health, School of Dental Medicine, Department of Orthodontics, School of Dental Medicine, and Center for Innovation & Precision Dentistry, School of Dental Medicine, School of Engineering and Applied Sciences, University of Pennsylvania, Philadelphia, Pennsylvania 19104, United States

**Abstract**

Severe tooth decay has been associated with iron deficiency anemia that disproportionately burdens susceptible populations. Current modalities are insufficient in severe cases where pathogenic dental biofilms rapidly accumulate, requiring new antibiofilm approaches. Here, we show that ferumoxytol, a Food and Drug Administration-approved nanoparticle formulation for treating iron deficiency, exerts an alternative therapeutic activity via the catalytic activation of hydrogen peroxide, which targets bacterial pathogens in biofilms and suppresses tooth enamel decay in an intraoral human disease model. Data reveal the potent antimicrobial specificity of ferumoxytol iron oxide nanoparticles (FerIONP) against biofilms harboring *Streptococcus mutans* via preferential binding that promotes bacterial killing through *in situ* free-radical generation. Further analysis indicates that the targeting mechanism involves interactions of FerIONP with pathogen-specific glucan-binding proteins, which have a minimal effect on commensal streptococci. In addition, we demonstrate that FerIONP can detect pathogenic biofilms on natural teeth via a facile colorimetric reaction. Our findings provide clinical evidence and the theranostic potential of catalytic nanoparticles as a targeted anti-infective nanomedicine.

**Graphical Abstract**



## Keywords

Iron oxide; nanozyme; antimicrobial; polymicrobial; dental caries; theranostics

## INTRODUCTION

Dental caries (tooth decay) is an unresolved public health problem that affects more than 2.3 billion people worldwide, particularly impoverished and medically compromised populations.<sup>1–3</sup> In particular, iron deficiency anemia is strongly associated with severe dental caries.<sup>4–8</sup> Current approaches are insufficient for susceptible populations, particularly in severe cases where pathogenic biofilms rapidly accumulate due to sugar-rich diets and poor oral hygiene and lead to the onset of caries that cannot be effectively controlled.<sup>9</sup> In caries-inducing (cariogenic) biofilms, microorganisms form highly organized and protected biostructures that create localized acidic pH microenvironments, promoting cariogenic bacteria growth and acid dissolution of the tooth enamel.<sup>10,11</sup> Available antimicrobial modalities are restricted to broad-spectrum agents that lack efficacy and targeting specificity against cariogenic biofilms and have limited effects against dental caries.<sup>12,13</sup> To overcome these challenges, new antibiofilm strategies are needed to target acidogenic properties under high cariogenic (sugar exposure and poor oral hygiene) conditions found in high-risk individuals.

Bioactive nanoparticles have shown remarkable versatility for targeting microbes in biofilms through multiple functionalities, ranging from enhanced penetration and drug delivery to on-demand activation in response to environmental stimuli.<sup>14–17</sup> Among them, catalytic iron oxide nanoparticles with enzyme-like properties (also termed nanozymes) are rapidly emerging due to their promising therapeutic activity in animal models.<sup>18,19</sup> We have reported that an iron oxide nanoparticle formulation known as ferumoxytol (FerIONP), which was approved by the Food and Drug Administration (FDA) for systemic use to treat iron deficiency, can disrupt cariogenic biofilms through acidic pH activation of hydrogen

peroxide via catalytic (peroxidase-like) activity when used topically in a rodent model.<sup>20</sup> However, its biological actions against biofilms formed in the human mouth are unknown, which would be critical to assess the targeting efficacy and clinical translatability of the FerIONP-based approach.

Here, we conducted a randomized crossover study whereby FerIONP treatments were performed on human subjects using a wearable intraoral appliance with implanted natural tooth enamel under severe conditions conducive of dental caries. We found that FerIONP displayed a potent antimicrobial specificity against biofilms harboring *Streptococcus mutans* (a cariogenic pathogen) but not against other oral bacteria, which resulted in the significant reduction of enamel demineralization. Further analyses revealed that FerIONP preferentially bound to *S. mutans* through a glucan-binding mechanism and selectively killed the pathogen through the localized generation of reactive oxygen species (ROS) *in situ*. In addition, we showed the possibility of using FerIONP for cariogenic biofilm detection using the catalytic mechanism. This dual functionality is summarized in Figure 1A. Together, we present the first human study demonstrating the potential therapeutic application of catalytic iron oxide nanoparticles (nanozymes) as a targeted nanomedicine against an oral infectious disease.

## RESULTS AND DISCUSSION

### FerIONP As an Antibiofilm and Caries Preventive Therapy.

To mimic the high-risk caries conditions in susceptible populations (high sugar intake and poor oral hygiene), we designed an intraoral model (Figure 1B) that allowed natural biofilm formation on the tooth enamel surface under frequent sucrose exposure without mechanical biofilm removal (brushing). In this model, treatments can be applied directly onto biofilm-covered enamel specimens and the entire intact samples can be recovered with minimal disturbance (Figure 1C), allowing the simultaneous evaluation of the localized (*in situ*) effects on biofilm accumulation and enamel demineralization. Furthermore, the specimens were exposed to a sugar (20% sucrose, v/v) solution four times a day with no mechanical cleaning (brushing) to mimic high-risk caries conditions (Figure 1C). We analyzed and compared the biological activity of the topical applications of FerIONP/H<sub>2</sub>O<sub>2</sub> (twice daily; after breakfast and before bedtime) with a vehicle control and with H<sub>2</sub>O<sub>2</sub> alone. The topical FerIONP dosage (1.5 mg per day) was based on previous *in vivo* and preliminary studies and was 340× less than the FDA-approved dose for systemic use (intravenous injection). The low amounts of FerIONP used here efficiently catalyze hydrogen peroxide (H<sub>2</sub>O<sub>2</sub>) at an acidic pH via peroxidase-like activity (Figure 1A and Figure S1). FerIONP alone was not included because it is inactive, as determined in both laboratory and rodent models.<sup>20</sup> The subjects wore the custom-fit appliances with enamel specimens in place for three treatment periods (Figure 1D, Figure S2A) and were monitored for adverse effects and compliance at each visit (Figure S2B). There were no reported complications or adverse events associated with the treatment (Figure S3).

At the end of each study period, the intraoral appliances were removed, and the biofilms were subjected to microbiological (viable cells) and confocal imaging (spatial organization) analyses.<sup>20,21</sup> We found no effect on the number of total viable cells in the biofilms treated with FerIONP/H<sub>2</sub>O<sub>2</sub> (Figure 2A). Our previous study showed potent killing activity toward

cariogenic species *in vitro*, particularly *S. mutans*,<sup>22</sup> suggesting selective antimicrobial activity. To explore this possibility, we analyzed a subset of the data from subjects who had *S. mutans* detected at the baseline. Remarkably, we observed that *S. mutans* was completely eradicated from biofilms treated with FerIONP/H<sub>2</sub>O<sub>2</sub> (Figure 2B). Confocal images also confirmed the microbiological data showing that biofilms harboring *S. mutans* cells (in green) were effectively inhibited (Figures 2C) after FerIONP/H<sub>2</sub>O<sub>2</sub> treatment, suggesting the targeting specificity against this organism.

Next, we evaluated the effect of FerIONP/H<sub>2</sub>O<sub>2</sub> on tooth enamel demineralization (decay) using the surface microhardness (SMH) analysis. Only FerIONP/H<sub>2</sub>O<sub>2</sub> significantly reduced the level of demineralization compared to the vehicle control (Figure 2D) despite the high cariogenic challenge induced by daily sucrose exposure. The therapeutic effect was more pronounced in individuals with *S. mutans* carriage (Figure 2E). This is particularly noteworthy because individuals with *S. mutans* displayed higher levels of enamel demineralization. Altogether, the data show antibiofilm and anticaries properties of FerIONP/H<sub>2</sub>O<sub>2</sub> under severe cariogenic conditions in humans. Moreover, FerIONP/H<sub>2</sub>O<sub>2</sub> displays a more targeted therapeutic effect on subjects harboring *S. mutans*, a cariogenic pathogen commonly found in severe cases of dental caries.<sup>23,24</sup>

### FerIONP Binds and Preferentially Kills *S. mutans* via *In Situ* H<sub>2</sub>O<sub>2</sub> Catalysis.

Given the potential targeting effect of FerIONP/H<sub>2</sub>O<sub>2</sub>, we hypothesized that (1) FerIONP could preferentially bind to *S. mutans* compared to other species and (2) thereby produce ROS in close proximity to more effectively kill this organism at an acidic pH. To probe these questions, we incubated FerIONP (1 mg/mL) with *S. mutans* or other oral commensal streptococci, including *Streptococcus oralis*, *Streptococcus gordonii*, and *Streptococcus sanguinis*, and assessed their binding profiles. As seen in Figure 3A, FerIONP bound significantly more to *S. mutans* compared to other strains, indicating a higher binding affinity to *S. mutans*. We also tested *Actinomyces naeslundii* (a nonstreptococcal species) and found a similar outcome (Figure S4). Cell viability was also assessed with the addition of H<sub>2</sub>O<sub>2</sub> after the incubation of FerIONP. The data showed that enhanced binding resulted in more effective bacterial killing of *S. mutans* after exposure to H<sub>2</sub>O<sub>2</sub> (>4-log reduction in viable counts compared to the control, Figure 3B), while the other species were not substantially affected.

The differences in FerIONP binding and subsequent killing may be due to the interactions between FerIONP and *S. mutans*' surface proteins. FerIONP is a nanoparticle comprised of an iron oxide core coated with carboxymethyl-dextran, which could bind specifically to *S. mutans* as this organism expresses several cell membrane-associated glucan-binding proteins.<sup>25,26</sup> At least two glucan-binding proteins (Gbps; GbpA and GbpC) other than glucosyltransferases (Gtfs, particularly GtfB and GtfC) with a glucan-binding domain are uniquely expressed in high levels by *S. mutans*, which can directly mediate binding interactions with dextran or dextran-coated surfaces.<sup>25,27,28</sup> To assess this hypothesis, we used Gbp and Gtf mutant strains of *S. mutans* to examine the FerIONP binding capacity. We found that the bacterial binding of FerIONP was significantly reduced, with much lower amounts of iron bound to either the Gbp or Gtf mutant strains compared to the

wild types (Figure 3C). Interestingly, the deletion of either GbpA or GbpC significantly impaired FerIONP binding to *S. mutans*. GbpA is a secreted protein associated with the cell surface, while GbpC appears to be anchored to the cell wall.<sup>25</sup> GbpA contains a high percentage of  $\beta$ -sheets in the carboxyl-terminal region, which may provide optimal folding and facilitate binding to glucans.<sup>25</sup> Conversely, GbpC shares structural similarities with the V region of antigen I/II and harbors unique loop regions in the lectin-like  $\beta$ -supersandwich fold that allow specific dextran binding with a high affinity.<sup>29</sup> Thus, the dextran binding interactions mediated by GbpA and GbpC may be distinctive but equally effective. Whether the deletion of GbpC can affect GbpA protein synthesis and secretion or the glucan binding affinity and vice versa remains to be elucidated, which may provide further insights on the FerIONP binding mechanism. Nevertheless, our findings can partially explain the enhanced pathogen killing by FerIONP/H<sub>2</sub>O<sub>2</sub> since its preferential binding to *S. mutans* would result in localized ROS generation in close proximity to the bacterial cell, especially given that ROS has a brief lifespan<sup>30,31</sup> and does not diffuse over long distances.<sup>32</sup>

To further elucidate the selective bacterial killing, we employed high-resolution fluorescence imaging with the simultaneous analysis of cell viability and ROS generation *in situ*. To visualize the distribution of live and dead bacteria, intact bacteria were labeled with SYTO 60, and propidium iodide (PI) was used to determine nonviable cells. For ROS, we used a fluorescent probe, hydroxyphenyl fluorescein (HPF), to detect hydroxyl radicals.<sup>22</sup> FerIONP (1 mg/mL) was added to an actively growing bacterial cells (*S. mutans* or *S. oralis*), which were exposed to H<sub>2</sub>O<sub>2</sub> and then observed using confocal microscopy. We found that most *S. mutans* cells were killed (in red) after treatment with FerIONP/H<sub>2</sub>O<sub>2</sub>, which was accompanied by the generation of large amounts of ROS (in purple) *in situ* (Figure 3D). In contrast, only a small proportion of *S. oralis* cells were affected, and much fewer ROS were observed. Interestingly, the spatial distribution of ROS signals matched the position of the dead cells, indicating that bacterial killing mainly originated from the oxidative damage. Consistent with our confocal findings, quantitative analysis confirmed that most of the *S. mutans* cells were killed (Figure 3E) with a large amount of ROS (Figure 3F) compared to *S. oralis*. These findings indicate that FerIONP displays a two-prong mode of action. (1) FerIONP binds with a higher specificity to *S. mutans* than to other species, which (2) allows H<sub>2</sub>O<sub>2</sub> catalysis on-site (directly on the bacterial surface) to produce antimicrobial free radicals *in situ*. This mechanism is important for the targeting specificity as the poor binding of FerIONP to commensal streptococci (which can produce H<sub>2</sub>O<sub>2</sub>) would also protect them against self-killing. Hence, a key concept is the “selective binding and enhanced *S. mutans* killing” via the peroxidase-like activity of FerIONP, which targets the pathogen while sparing the commensals in the presence of H<sub>2</sub>O<sub>2</sub>.

### FerIONP Detects Pathogenic Biofilms.

Given the preferential binding to *S. mutans* and H<sub>2</sub>O<sub>2</sub> catalysis at an acidic pH, FerIONP could be used for cariogenic biofilm detection. To test this possibility, we employed a biofilm model using *S. mutans* and *S. oralis* grown on saliva-coated hydroxyapatite discs as single or mixed-species biofilms. For the mixed-species system, the microorganisms were grown under high- or low-sugar conditions, which generated acidic or nonacidic biofilms, respectively.<sup>33</sup> Single and mixed-species biofilms were treated with FerIONP (1

mg/mL) and washed to removed unbound material, which was immediately followed by a colorimetric assay using 3,3',5,5'-tetramethyl-benzidine (TMB). FerIONP can oxidize colorless TMB (via free-radical generation from H<sub>2</sub>O<sub>2</sub> catalysis) to blue colored reaction products that can be quantified by measuring the absorbance at 652 nm.<sup>20</sup> We found that *S. mutans* biofilms exhibit readily visible blue staining with significantly higher absorbance levels (Figure 4A) than those of the biofilms harboring *S. oralis*. This observation was further confirmed in mixed-species biofilms grown in high-sugar (acidogenic) conditions and enriched with *S. mutans* (versus low-sugar conditions with a high proportion of *S. oralis*, Figure 4B). Using a human tooth model (Figure 4C), we observed similar blue staining of *S. mutans* biofilms formed on natural teeth under cariogenic conditions (high-sugar and acidic pH), indicating the diagnostic potential of FerIONP.

Previous investigations have shown that catalytic iron oxide nanoparticles (also termed nanozymes) display antimicrobial and antibiofilm properties *in vitro* and in animal models.<sup>19,34</sup> However, to the best of our knowledge nanozymes have yet to be tested in humans, which can further elucidate their bioactivity and targeting properties. Here, we show that FerIONP operates at low dose through a selective binding-activation mechanism to disrupt pathogenic biofilms and suppress tooth enamel demineralization under severe conditions in the human mouth. Importantly, neither adverse signs in the oral cavity nor systemic reactions were observed during the treatment periods. These findings can motivate its path to clinical translation for caries prevention, which is particularly relevant given that current approaches are insufficient for susceptible populations where cariogenic biofilms cannot be effectively controlled.

Despite promising findings, we emphasize the limitations of this study but also the opportunities for future research. Limitations include the short clinical duration, the limited characterization of the microbial composition, and the end-point data analysis. Long-term clinical studies with a larger number of samples collected longitudinally combined with multilabeling and multiomics approaches may reveal how topical FerIONP affects biofilm development at various spatial, temporal, and phylogenetic scales. Such in-depth analyses could further elucidate its antimicrobial specificity mechanisms and identify additional therapeutic targets. Furthermore, the flexibility of FerIONP chemistry provides interesting possibilities for improvement, such as chemically doping the iron oxide core with remineralizing agents like calcium fluoride or exploiting the dextran coating to conjugate biologics (enzymes or antimicrobial peptides) for enhanced catalytic and therapeutic performance as shown recently.<sup>22</sup>

An immediate application of FerIONP is related to the association of iron deficiency anemia with aggressive dental caries.<sup>4-6,35,36</sup> The common risk factors linked with severe childhood caries and iron deficiency include a high dietary sugar intake, malnutrition, and poor oral hygiene.<sup>8,9,37,38</sup> High sucrose consumption and poor oral care promotes the accumulation of acidogenic biofilms often enriched with *S. mutans*.<sup>11,33</sup> The preferential binding of FerIONP to *S. mutans* and its catalytic activation at an acidic pH are advantageous in severe cariogenic conditions without affecting commensals, which can provide a more targeted approach. As FerIONP has been used in children and adults,<sup>39,40</sup> it opens the possibility to

employ these FDA-approved nanoparticles for caries prevention tailored to high-risk patients with iron deficiency anemia.

Interestingly, optimal levels of iron in saliva may also provide protective effects against dental caries.<sup>41</sup> Iron ions can precipitate on the enamel surface as thin acid-resistant coatings and promote calcium and phosphate adsorption, reducing enamel demineralization. However, FerIONP releases negligible amounts of free iron, even under acidic pH (pH 4.5) conditions, both in solution and within biofilms.<sup>20</sup> Conversely, effective biofilm inhibition can potentiate the anticaries effects of fluoride on enamel remineralization.<sup>33</sup> Whether topical FerIONP with iron or fluoride supplementation can synergistically enhance protective effects in susceptible individuals awaits further investigation. Given this oral-systemic relationship, clinical trials could explore whether repeated topical oral applications of FerIONP in conjunction with its systemic use can help reduce iron deficiency and prevent severe childhood caries, two major unresolved global health problems.<sup>42,43</sup>

## Supplementary Material

Refer to Web version on PubMed Central for supplementary material.

## ACKNOWLEDGMENTS

This study was supported by NIH Grant R01DE025848. Additional support was provided by Johnson & Johnson (no. 573399).

## REFERENCES

- (1). GBD 2017 Oral Disorders Collaborators. Global, regional, and national levels and trends in burden of oral conditions from 1990 to 2017: A systematic analysis for the global burden of disease 2017 study. *J. Dent. Res* 2020, 99 (4), 362–373. [PubMed: 32122215]
- (2). Watt RG; Daly B; Allison P; Macpherson LMD; Venturelli R; Listl S; Weyant RJ; Mathur MR; Guarnizo-Herreno CC; Celeste RK; Peres MA; Kearns C; Benzian H Ending the neglect of global oral health: Time for radical action. *Lancet* 2019, 394 (10194), 261–272. [PubMed: 31327370]
- (3). Peres MA; Macpherson LMD; Weyant RJ; Daly B; Venturelli R; Mathur MR; Listl S; Celeste RK; Guarnizo-Herreno CC; Kearns C; Benzian H; Allison P; Watt RG Oral diseases: A global public health challenge. *Lancet* 2019, 394 (10194), 249–260. [PubMed: 31327369]
- (4). Shaoul R; Gaitini L; Kharouba J; Darawshi G; Maor I; Somri M The association of childhood iron deficiency anaemia with severe dental caries. *Acta Paediatr.* 2012, 101 (2), e76–e79. [PubMed: 21883449]
- (5). Schroth RJ; Levi J; Kliewer E; Friel J; Moffatt ME Association between iron status, iron deficiency anaemia, and severe early childhood caries: A case-control study. *BMC Pediatr.* 2013, 13,22. [PubMed: 23388209]
- (6). Bansal K; Goyal M; Dhingra R Association of severe early childhood caries with iron deficiency anemia. *J. Indian Soc. Pedod. Prev. Dent* 2016, 34 (1), 36–42. [PubMed: 26838146]
- (7). Deane S; Schroth RJ; Sharma A; Rodd C Combined deficiencies of 25-hydroxyvitamin D and anemia in preschool children with severe early childhood caries: A case-control study. *Paediatr. Child Health* 2018, 23 (3), e40–e45. [PubMed: 29769814]
- (8). Gurunathan D; Swathi A; Kumar MS Prevalence of iron deficiency anemia in children with severe early childhood caries. *Biomed. Pharmacol. J* 2019, 12 (1), 219–225.
- (9). Anil S; Anand PS Early childhood caries: Prevalence, risk factors, and prevention. *Front Pediatr.* 2017, 5, 157. [PubMed: 28770188]



- (10). Hajishengallis E; Parsaei Y; Klein MI; Koo H Advances in the microbial etiology and pathogenesis of early childhood caries. *Mol. Oral Microbiol* 2017, 32 (1), 24–34. [PubMed: 26714612]
- (11). Bowen WH; Burne RA; Wu H; Koo H Oral biofilms: Pathogens, matrix, and polymicrobial interactions in microenvironments. *Trends Microbiol.* 2018, 26 (3), 229–242. [PubMed: 29097091]
- (12). Autio-Gold J The role of chlorhexidine in caries prevention. *Oper. Dent* 2008, 33 (6), 710–716. [PubMed: 19051866]
- (13). Arweiler NB Oral mouth rinses against supragingival biofilm and gingival inflammation. *Monogr. Oral Sci* 2021, 29, 91–97. [PubMed: 33427225]
- (14). Besinis A; De Peralta T; Tredwin CJ; Handy RD Review of nanomaterials in dentistry: Interactions with the oral micro-environment, clinical applications, hazards, and benefits. *ACS Nano* 2015, 9 (3), 2255–2289. [PubMed: 25625290]
- (15). Koo H; Allan RN; Howlin RP; Stoodley P; Hall-Stoodley L Targeting microbial biofilms: current and prospective therapeutic strategies. *Nat. Rev. Microbiol* 2017, 15 (12), 740–755. [PubMed: 28944770]
- (16). Benoit DS; Sims KR Jr; Fraser D Nanoparticles for oral biofilm treatments. *ACS Nano* 2019, 13 (5), 4869–4875. [PubMed: 31033283]
- (17). Liu Y; Shi L; Su L; van der Mei HC; Jutte PC; Ren Y; Busscher HJ Nanotechnology-based antimicrobials and delivery systems for biofilm-infection control. *Chem. Soc. Rev* 2019, 48 (2), 428–446. [PubMed: 30601473]
- (18). Cormode DP; Gao L; Koo H Emerging biomedical applications of enzyme-like catalytic nanomaterials. *Trends Biotechnol.* 2018, 36 (1), 15–29. [PubMed: 29102240]
- (19). Wu J; Wang X; Wang Q; Lou Z; Li S; Zhu Y; Qin L; Wei H Nanomaterials with enzyme-like characteristics (nanozymes): Next-generation artificial enzymes (II). *Chem. Soc. Rev* 2019, 48 (4), 1004–1076. [PubMed: 30534770]
- (20). Liu Y; Naha PC; Hwang G; Kim D; Huang Y; Simon-Soro A; Jung HI; Ren Z; Li Y; Gubara S; Alawi F; Zero D; Hara A; Cormode DP; Koo H Topical ferumoxytol nanoparticles disrupt biofilms and prevent tooth decay *in vivo* via intrinsic catalytic activity. *Nat. Commun* 2018, 9 (1), 2920. [PubMed: 30065293]
- (21). Kim D; Barraza JP; Arthur RA; Hara A; Lewis K; Liu Y; Scisci EL; Hajishengallis E; Whiteley M; Koo H Spatial mapping of polymicrobial communities reveals a precise biogeography associated with human dental caries. *Proc. Natl. Acad. Sci. U. S. A* 2020, 117 (22), 12375–12386. [PubMed: 32424080]
- (22). Huang Y; Liu Y; Shah S; Kim D; Simon-Soro A; Ito T; Hajfathalian M; Li Y; Hsu JC; Nieves L; Alawi F; Naha PC; Cormode DP; Koo H Precision targeting of bacterial pathogen via bi-functional nanozyme activated by biofilm microenvironment. *Biomaterials* 2021, 268, 120581. [PubMed: 33302119]
- (23). Abranches J; Zeng L; Kajfasz JK; Palmer SR; Chakraborty B; Wen ZT; Richards VP; Brady LJ; Lemos JA Biology of oral streptococci. *Microbiol. Spectrum* 2018, 6 (5), 6.5.11 DOI: 10.1128/microbiolspec.GPP3-0042-2018.
- (24). Parisotto TM; Steiner-Oliveira C; Silva CM; Rodrigues LK; Nobre-dos-Santos M Early childhood caries and mutans streptococci: A systematic review. *Oral Health Prev. Dent* 2010, 8 (1), 59–70. [PubMed: 20480056]
- (25). Banas J; Vickerman M Glucan-binding proteins of the oral streptococci. *Crit. Rev. Oral Biol. Med* 2003, 14 (2), 89–99. [PubMed: 12764072]
- (26). Matsumoto-Nakano M Role of *Streptococcus mutans* surface proteins for biofilm formation. *Jpn. Dent. Sci. Rev* 2018, 54 (1), 22–29. [PubMed: 29628998]
- (27). Lynch DJ; Fountain TL; Mazurkiewicz JE; Banas JA Glucan-binding proteins are essential for shaping *Streptococcus mutans* biofilm architecture. *FEMS Microbiol. Lett* 2007, 268 (2), 158–165. [PubMed: 17214736]
- (28). Lynch DJ; Michalek SM; Zhu M; Drake D; Qian F; Banas JA Cariogenicity of *Streptococcus mutans* glucan-binding protein deletion mutants. *Oral Health Dent. Manag* 2013, 12 (4), 191–199. [PubMed: 24390015]

- (29). Mieher JL; Larson MR; Schormann N; Purushotham S; Wu R; Rajashankar KR; Wu H; Deivanayagam C Glucan binding protein C of *Streptococcus mutans* mediates both sucrose-independent and sucrose-dependent adherence. *Infect. Immun* 2018, 86 (7), e00146. [PubMed: 29685986]
- (30). Koppenol W The reaction of ferrous EDTA with hydrogen peroxide: evidence against hydroxyl radical formation. *J. Free Radicals Biol. Med* 1985, 1 (4), 281–285.
- (31). Attri P; Kim YH; Park DH; Park JH; Hong YJ; Uhm HS; Kim KN; Fridman A; Choi EH Generation mechanism of hydroxyl radical species and its lifetime prediction during the plasma-initiated ultraviolet (UV) photolysis. *Sci. Rep* 2015, 5 (1), 9332. [PubMed: 25790968]
- (32). Guo Q; Yue Q; Zhao J; Wang L; Wang H; Wei X; Liu J; Jia J How far can hydroxyl radicals travel? An electrochemical study based on a DNA mediated electron transfer process. *Chem. Commun* 2011, 47 (43), 11906–11908.
- (33). Pitts NB; Zero DT; Marsh PD; Ekstrand K; Weintraub JA; Ramos-Gomez F; Tagami J; Twetman S; Tsakos G; Ismail A Dental caries. *Nat. Rev. Dis. Primers* 2017, 3, 17030. [PubMed: 28540937]
- (34). Huang Y; Ren J; Qu X Nanozymes: classification, catalytic mechanisms, activity regulation, and applications. *Chem. Rev* 2019, 119 (6), 4357–4412. [PubMed: 30801188]
- (35). Iranna Koppal P; Sakri MR; Akkareddy B; Hinduja DM; Gangolli RA; Patil BC Iron deficiency in young children: a risk marker for early childhood caries. *Int. J. Clin. Pediatr. Dent* 2013, 6(1), 1–6. [PubMed: 25206178]
- (36). Tang R; Huang M; Huang S Relationship between dental caries status and anemia in children with severe early childhood caries. *Kaohsiung J. Med. Sci* 2013, 29 (6), 330–336. [PubMed: 23684139]
- (37). Acs G; Lodolini G; Kaminsky S; Cisneros GJ Effect of nursing caries on body weight in a pediatric population. *Pediatr. Dent* 1992, 14 (5), 302–305. [PubMed: 1303533]
- (38). Colak H; Dulgergil CT; Dalli M; Hamidi MM Early childhood caries update: A review of causes, diagnoses, and treatments. *J. Nat. Sci. Biol. Med* 2013, 4 (1), 29–38. [PubMed: 23633832]
- (39). Hassan N; Boville B; Reischmann D; Ndika A; Sterken D; Kovey K Intravenous ferumoxytol in pediatric patients with iron deficiency anemia. *Ann. Pharmacother* 2017, 51 (7), 548–554. [PubMed: 28622742]
- (40). Auerbach M; Chertow GM; Rosner M Ferumoxytol for the treatment of iron deficiency anemia. *Expert Rev. Hematol* 2018, 11(10), 829–834. [PubMed: 30188740]
- (41). Torell P Iron and dental caries. *Swed. Dent. J* 1988, 12 (3), 113–124. [PubMed: 3165568]
- (42). GBD 2015 Oral Health Collaborators. Global, regional, and national prevalence, incidence, and disability-adjusted life years for oral conditions for 195 countries, 1990–2015: A systematic analysis for the global burden of diseases, injuries, and risk factors. *J. Dent. Res* 2017, 96 (4), 380–387. [PubMed: 28792274]
- (43). GBD 2015 Disease and Injury Incidence and Prevalence Collaborators. Global, regional, and national incidence, prevalence, and years lived with disability for 310 diseases and injuries, 1990–2015: A systematic analysis for the global burden of disease study 2015. *Lancet* 2016, 388 (10053), 1545–1602. [PubMed: 27733282]

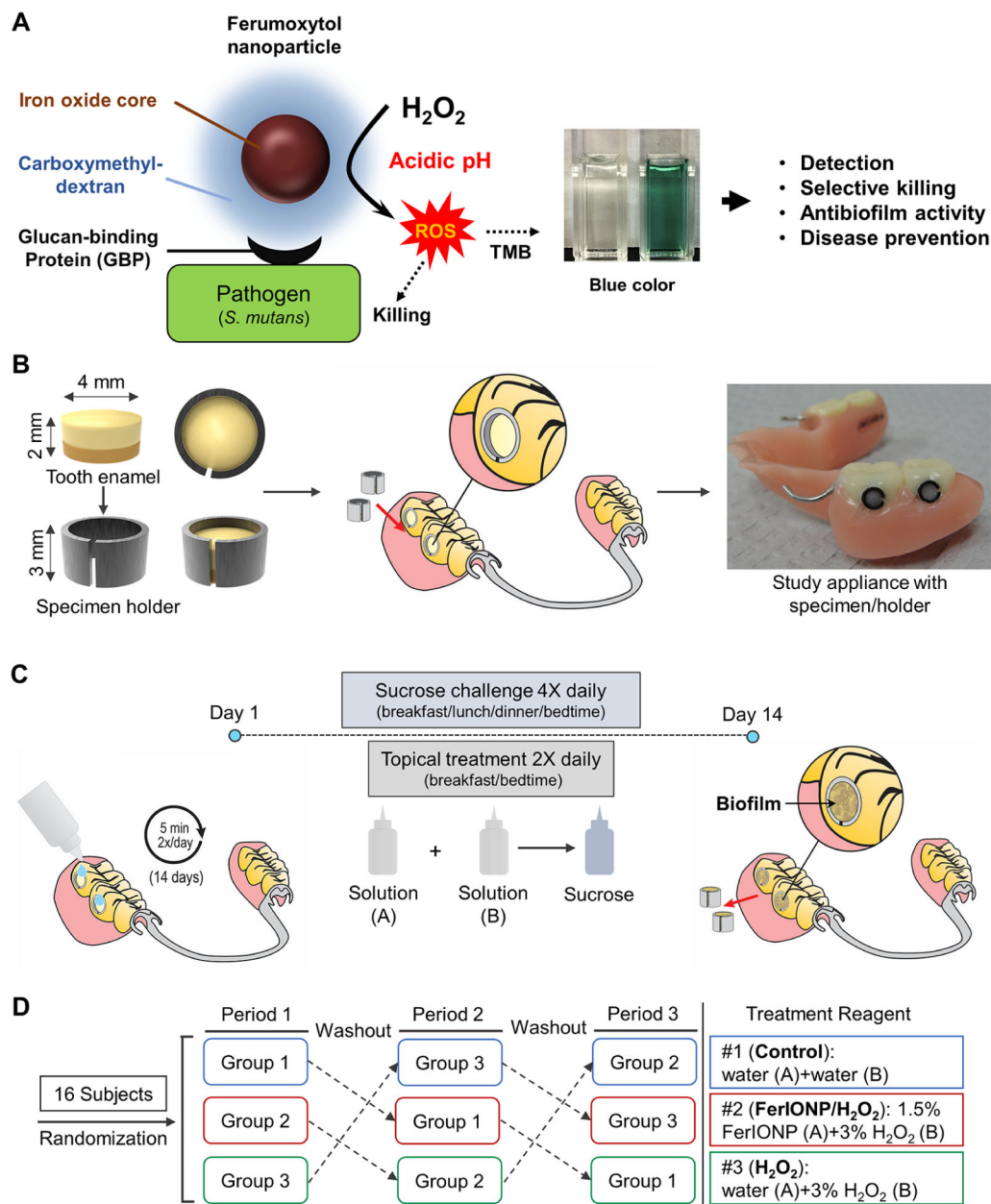


**Figure 1.**

Intraoral human biofilm disease model and treatment regimen. (A) Schematic depiction of the selective catalytic-therapeutic-diagnostic mechanism of FerIONP. (B) Tooth enamel specimen placed in a custom-fit holder assembly that can be implanted in a wearable and personalized partial denture. (C) Treatment regimen. The subjects were instructed to drip one drop from solution bottle A onto each specimen, wait for 5 min, then immediately drip one drop from solution bottle B onto each specimen and wait for an additional 5 min. The concentration of  $H_2O_2$  in solution B was 3%, but we added solution B after the solution A treatment at a 1:1 ratio. Thus, the final concentration for  $H_2O_2$  during the procedure was 1.5%. This was followed by applying a 20% sucrose solution onto the specimens for 3 min to provide a cariogenic challenge. (D) Randomized crossover design with three test periods

utilizing 16 subjects. At each study period, subjects received different treatment products, followed by a one-week washout period. All the data were collected from 15 participants since one subject lost the partial denture.

Author Manuscript

Author Manuscript

Author Manuscript

Author Manuscript

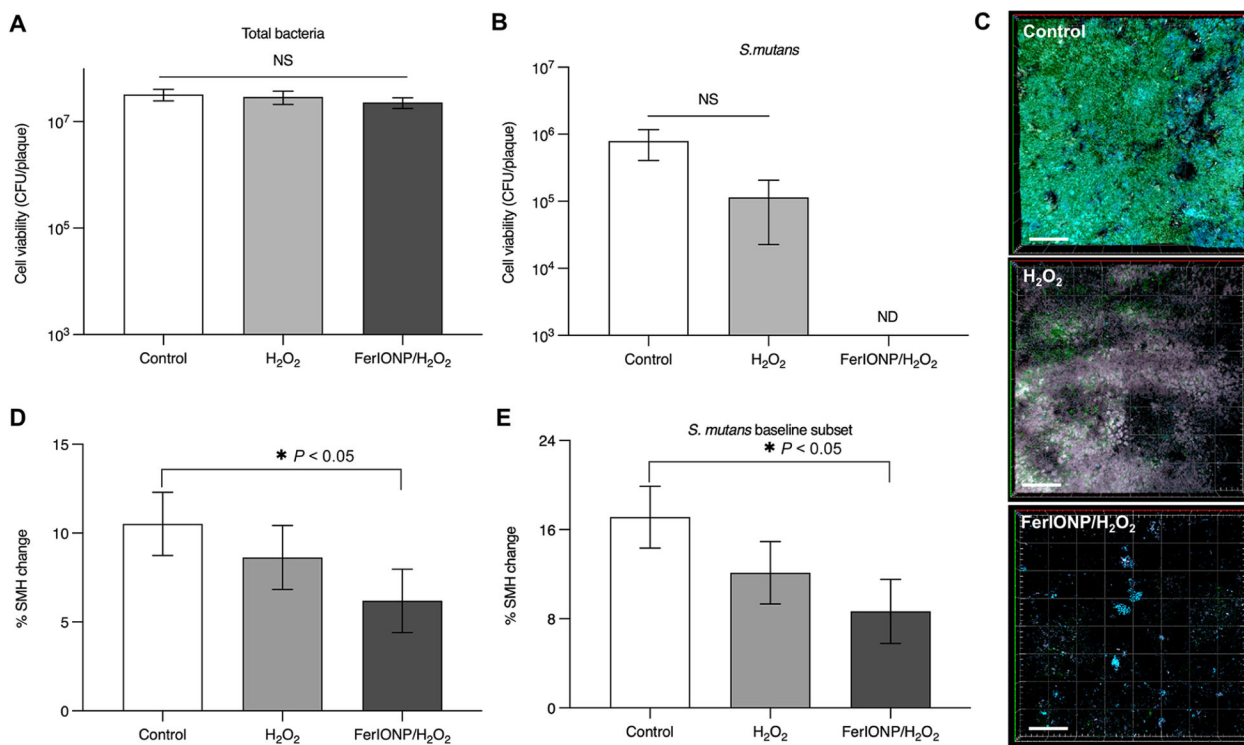


**Figure 2.**

Biofilm and tooth-enamel analysis. Viable cell counts (CFU) of (A) the total bacteria ( $n = 15$ ) and (B) *S. mutans* ( $n = 6$ ; subset of *S. mutans* positive at the baseline) recovered from the *in situ* biofilms. (C) Confocal images of representative intact biofilms on enamel surfaces following the treatments. FISH oligonucleotide probes were used for *S. mutans* (MUT590, 5'-ACTCCAGACTTTCCTGAC-3' with Alexa Fluor 488), as shown in green, and for all bacteria (EUB338, 5'-GCTGCTCCCGTAGGATG-3' with Cy3), as indicated in blue. The scale bar is 50  $\mu\text{m}$ . (D) Surface microhardness change (% SMHC) for the enamel specimens ( $n = 15$ ); % SMH change =  $[(D1 - B)/(B)] \times 100$ , where  $B$  is the microhardness indentation length ( $\mu\text{m}$ ) of a sound enamel specimen at the baseline and  $D1$  is the microhardness indentation length ( $\mu\text{m}$ ) after demineralization. (E) Graph of the % SMHC for the subset with *S. mutans* at the baseline ( $n = 6$ ). The analysis was performed with a one-way analysis of variance (ANOVA,) followed by either Tukey's posthoc test or the Kruskal-Wallis test for multiple comparison. All values are reported as mean  $\pm$  SD, \* $P < 0.05$ ; NS stands for not significant, and ND stands for not detectable.

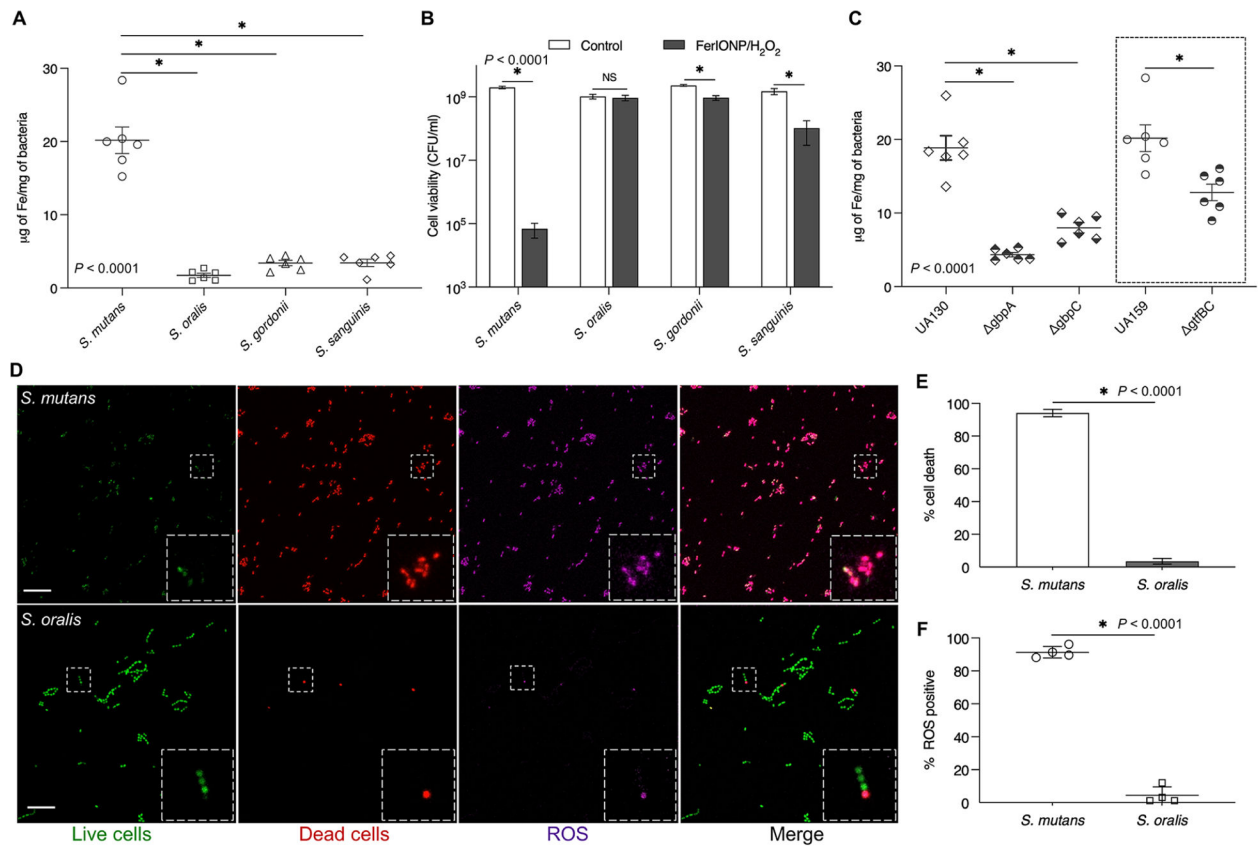


**Figure 3.** Preferential pathogen-binding and killing by FerIONP. (A) FerIONP binding to different oral streptococci ( $n = 6$ ). (B) Killing efficacy of FerIONP/H<sub>2</sub>O<sub>2</sub> against *S. mutans* and other commensals ( $n = 6$ ). (C) FerIONP binding to *S. mutans* wild type (UA159 or UA130) and Gbp or Gtf mutant strains ( $n = 6$ ). (D) *In situ* ROS generation and killing effect of *S. mutans* compared to *S. oralis*. Live cells were stained with SYTO 60 (green), dead cells were stained with PI (red), and ROS were labeled using HPF (purple). HPF stands for hydroxyphenyl fluorescein. The scale bar is 10  $\mu$ m. (E) Quantitative analysis of dead cells and (F) ROS generation ( $n = 4$ ). The analysis was performed with a one-way analysis of variance (ANOVA), followed by Tukey's posthoc test for a multiple comparison (A and C) or Student's *t*-test (B, E, and F). All values are reported as mean  $\pm$  SD, \* $P < 0.0001$ ; NS stands for not significant.

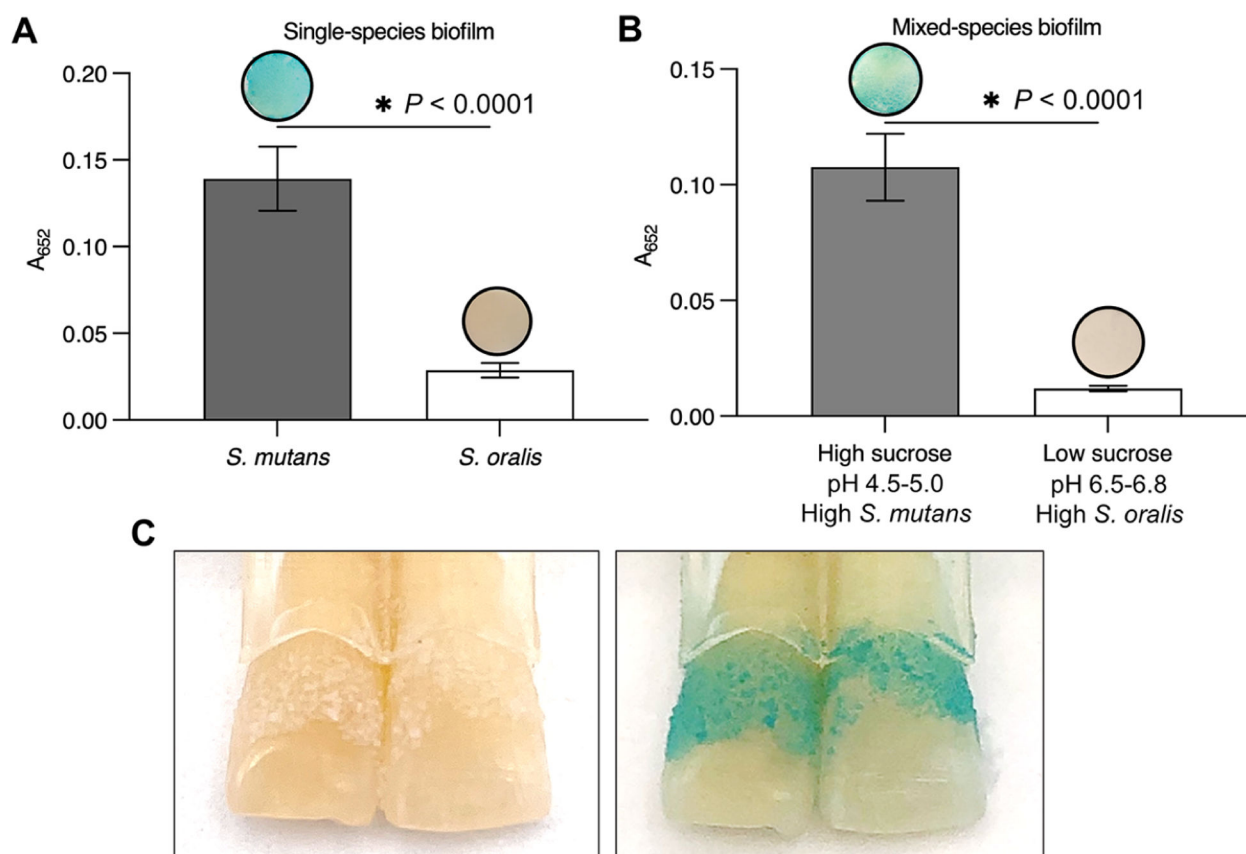


**Figure 4.** FerIONP detects pathogenic biofilms. (A) *S. mutans* biofilms were stained in blue by the FerIONP (vs *S. oralis* biofilms) catalysis of H<sub>2</sub>O<sub>2</sub> via a colorimetric reaction using 3,3',5,5'-tetramethylbenzidine (TMB). For the colorimetric assay, 1% H<sub>2</sub>O<sub>2</sub> was used, which provided an optimal quantitative measurement at an absorbance of 652 nm (as well as clear visualization) within the 5 min reaction time. (B) Similar blue staining was observed in mixed-species biofilms formed with high-sucrose (1%) and a high proportion of *S. mutans* (>90%) compared to low-sucrose (0.1%) and a low proportion of *S. mutans* (<10%) ( $n = 4$ ). Differences between groups were assessed by Student's *t*-test. All values are reported as mean ± SD, \* $P < 0.0001$ . (C) FerIONP can detect biofilms formed on natural teeth.